The Effect of Pulsed Current and Organic Additives on Hydrogen Incorporation in Electroformed Copper Used in Ultrahigh Vacuum Applications

L. Lain Amador, J. Rolet, M.-L. Doche, P. Massuti-Ballester, M.-P. Gigandet, V. Moutarlier, M. Taborelli, L. Ferreira, P. Chiggiato, J.-Y. Hihn

Journal of The Electrochemical Society

The Effect of Pulsed Current and Organic Additives on Hydrogen Incorporation in Electroformed Copper Used in Ultrahigh Vacuum Applications

The Effect of Pulsed Current and Organic Additives on Hydrogen Incorporation in Electroformed Copper Used in Ultrahigh Vacuum Applications

L. Lain Amador,[1,2] J. Rolet,[2,3] M-L Doche,[2] P. Massuti-Ballester,[1] M-P Gigandet,[2] V. Moutarlier,[2] M. Taborelli,[1] L. M. A. Ferreira,[1] P. Chiggiato,[1] and J-Y Hihn [2,*,z]

[1] *CERN, European Organization for Nuclear Research, CH-1211 Geneva 23, Switzerland*
[2] *UTINAM, UMR 6213 CNRS, Besançon Univ. Bourgogne Franche Comte, F-25030 Besançon, France*
[3] *IRT M2P, F-57070 Metz, France*

The presence of hydrogen in electroformed copper from two different acidic copper sulfate solutions was evaluated: an additive-free solution and a solution including a sugar. D-xylose addition is found to inhibit H incorporation and allows the use of higher cathodic pulses before the copper diffusion limited range starts. TDS experiments show that hydrogen is trapped in the copper samples in two different forms. Hydrogen diffused from copper vacancies was found on all samples at an outgassing temperature of around 450°C. For samples with long pulse times, an additional H_2 outgassing peak was found at around 600°C. XRD measurements allowed us to determine the preferential orientation of the plated samples and to monitor lattice parameter evolution with increasing temperature.
 [DOI: 10.1149/2.1211908jes]

Manuscript submitted November 2, 2018; revised manuscript received March 25, 2019. Published May 28, 2019. This was Paper 1261 presented at the Seattle, Washington Meeting of the Society, May 13–17, 2018.

The trend in synchrotron light source accelerator design consists in approaching the poles of the steering magnets closer to the electron beam. This implies reducing the bore hosting the vacuum chamber and using very small diameter vacuum pipes.[1] In order to maintain low pressure in these sections, non-evaporable getter thin film coatings are needed on the internal surface of vacuum chambers.[2,3] Application of functional thin films by physical vapor deposition in such small diameter and high aspect ratio chambers then becomes very difficult. A new approach relies on copper electroforming to build the vacuum chamber onto a pre-deposited thin film coating.[4] In this method, unlike the usual process, the pipe is built from the inside out. An aluminum mandrel is coated, first, with a functional thin film, then with a copper film and, finally, with a thick electroplated copper (1-3 mm) structural layer. In order to achieve extremely low pressures, the outgassing from the chamber has to be limited.[5] Replacement of high-purity copper parts by electroformed copper parts may nevertheless lead to the incorporation of various impurities including hydrogen, which is generated by solvent reduction and thus trapped in the coating.

Farmer et al.[6] reported instabilities during electroformed copper heat-treatment at 450°C, when a group of proprietary additives was used in the plating, and ascribed it to the presence of voids in the deposit. By contrast, copper electroplated from another acid copper solution with different proprietary additives contained no voids and could be safely heated at 1000°C. Gubin et al.[7] found that hydrogen can be present in different bound states and its concentration is found to be five to six orders of magnitude larger than the equilibrium solubility of hydrogen at room temperature. Thermal desorption spectroscopy studies on electrodeposited copper revealed a pronounced outgassing peak, which was ascribed to the break-up of vacancy–hydrogen clusters.[8]

Sulfur-free deposits, with carbon and nitrogen contents of about 0.015 to 0.003 and 0.001 wt%, respectively, were obtained from solutions containing polypropylene ether.[9] Other additives such as glue and phenol sulfonic were used to prepare high-throw acid copper solutions for electroforming of bellows.[10] Srivasta et al.[11] found that impurities decreased with the increase in plating temperature, the increase in acidity of the plating solution, and the addition of 0.1 $g.L^{-1}$ gelatin. In particular, low impurity deposits were found when pentoses were used as additives.[12] Moreover, the effect of the plating mode on the quality of electroplated copper deposits has also been studied. Pulse current is known to improve deposit morphology[13,14] and offers a large number of parameters for optimization (i.e. on-time, off-time, cathodic and anodic pulse, pulse duration). This technology has been the target of many research papers,[15–17] as well as of industrial applications protected by patents.[18,19] Its use in the case of copper electrodeposition and to the effect of pulse parameters on copper coatings properties (crystalline structure and grain size) has been until recently the subject of developments.[20]

The aim of the present study is the evaluation of the effect of two main triggers, namely polarization wave modulation and copper electrolyte composition, by the addition of organic additives on the hydrogen production and the possible further hydrogen incorporation in the electroplated deposit. D-xylose addition is chosen in this study because of its role as an oxygen control additive and its reported production of very pure copper deposits.[12,21,22]

Experimental

Two acidic copper sulfate electrolytes were prepared, made up of 115 $g.L^{-1}$ $CuSO_4.5H_2O$, 165 $g.L^{-1}$ H_2SO_4, and 0.075 $g.L^{-1}$ Cl^-. Additionally, in the second bath, d-xylose ($OCH-(CHOH)_3-CH_2OH$, pentose) was added in a very low concentration as shown in Table I.

A three-electrode cell is connected to a PRT 20–2 type potentiostat, used to impose a rectangular current pulse, from which transient curves in potential were derived by the addition of a resistance. A Scopix OX 7102-C oscilloscope is used to record the transient curves. The set-up comprises a rotating working electrode made of copper and rotating at a speed of 400 rpm, a Pt counter electrode, and a SCE electrode as reference. The pulse sequences were designed to deliver rectangular cathodic pulses with an amplitude ranging from 40 A dm^{-2} to 100 A dm^{-2}, for a given cathodic time of 100 ms (T_{on}). Time off (between the rectangular pulses) was adjusted to keep a constant average current of

Table I. Bath concentrations for the two electrolytes.

	Bath without additives	Bath with d-xylose
$CuSO_4 \cdot 5H_2O$ ($g.L^{-1}$)	115.0	115.0
H_2SO_4 ($g.L^{-1}$)	165.6	165.6
NaCl ($g.L^{-1}$)*	0.124	0.124
d-xylose ($g.L^{-1}$)	-	0.033
pH	0.3	0.3

*It is important to note that chloride content must be kept at the same level (0.075 $g.L^{-1}$) in the event of other Cl^- sources such as $CuCl_2$.

*Electrochemical Society Member.
[z]E-mail: jean-yves.hihn@univ-fcomte.fr

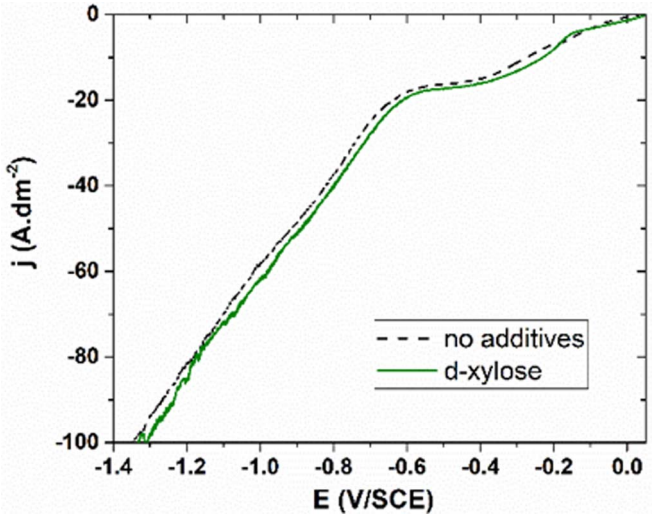

Figure 1. Cathodic polarization curve of $CuSO_4 + H_2SO_4$ bath without additives (dash line) and with 33 mg/L of d-xylose (solid line) – scan rate 10 mV/s.

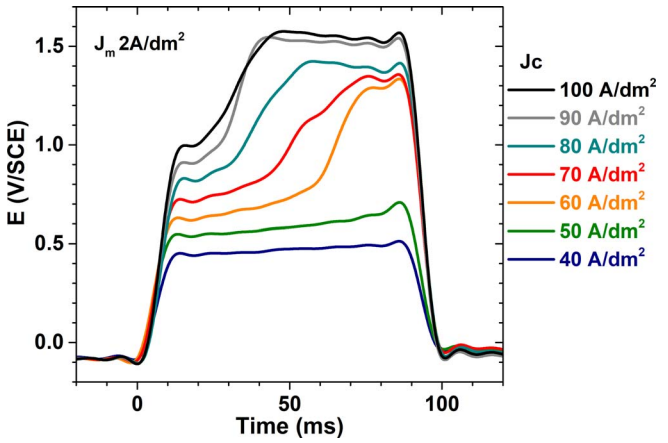

Figure 2. Transient curves in response to different cathodic currents (40–100 A dm^{-2}) for a fixed T_{on} = 100 ms, and constant $I_{average}$ = 2 A dm^{-2} recorded for the bath without additives.

2 A dm^{-2} ($J_{average} = J_{on}xT_{on}/(T_{on} \pm T_{off})$). Afterwards, electroformed samples were produced on aluminum platelet mandrels, which were pre-coated with a thin copper layer by physical vapor deposition. Electroforming was carried out in the two baths described using copper phosphorized anodes and magnetic stirring at a temperature of 25°C with a Micronics System LabPulse model with an output current range of −/+ 5 A and a voltage range of −/+ 10 V. To monitor the amount of incorporated hydrogen Thermal Desorption Spectroscopy analysis (TDS) was carried out in an ultra-high vacuum system (10^{-10} mbar range), which contains a sample holder to which a thermocouple and a heater are attached and a residual gas analyzer (RGA) which is placed above the sample. The gases desorbed during the thermal ramp are measured as a function of temperature by the calibrated RGA at a 10°C/min step rate from 20°C to 700°C. Sample size of 1cm x 1cm was required for the TDS measurements. Sample imaging was carried out using secondary electron microscopy (SEM).

The X-ray diffraction (XRD) experiments were conducted using a D8 Advance Bruker diffractometer, in Bragg-Brentano geometry. The in-situ high-temperature chamber consisted of a HTK 1200 ANTON PAAR cell. A Cu Kα source, operated at 40 kV and 40 mA, and a Ni filter were used. After an optimization study where the heating ramp varied from 10°C/min to 30°C/min, the lowest was chosen and samples were heated at 300°C, 500°C and 700°C at a measured ramp of 10°C/min in the diffractometer, which is in accordance with the TDS protocol. Measurements were carried out under vacuum (1 mbar). For the measurements, 2θ was used between 40 and 95°, with a step width of 0.02° and a scan speed of 0.3 s/step.

Results and Discussion

Pulse sequence design and response in transient curves.—Prior to transient curves determination, the cathodic behavior was recorded by Linear Sweep Voltammetry starting at the OCP (41 mV/SCE). Curves present a very similar behavior in the presence or absence of xylose, especially under -0,3 V/ECS, were the reaction is controlled by diffusion (Figure 1). It is possible to observe a slight current immediately after starting the LSV, which can be generated by reduction reactions at Under Potential Deposition, as it has been observed for some metals[23,24] or even hydrogen,[23] but the current levels remain always very low. The zone of interest starts above 20 A.dm^{-2} (−0.6 V/SCE), where the diffusional plateau ends and where a larger amount of hydrogen is produced, which is where the use of pulse sequence may be of interest to limit the competition between copper reduction and hydrogen production. It is interesting to note that, as soon as the copper reduction starts i.e. (−0.2 V/SCE), the current density is always higher in presence of D-xylose illustrating its effect of inducing copper growth.

Transient curves in response to pulsed currents were studied for various cathodic current densities. This technique is very sensitive to any system changes, because applied current densities are very high, pushing the system to its extreme values. Two main patterns were observed as shown for the base electrolyte (Figure 2) as well as in presence of xylose (Figure 3). At low current densities, i.e. below 50 A dm^{-2}, potential increases rapidly and reaches a constant value. For higher current densities, two characteristic plateaus can be observed: the first corresponds to the faradaic reduction of copper below the diffusion limit, while the second, at higher potential, is attributed to an increase of the local resistance induced by the depletion of the concentration of copper close to the interface. This situation called "diffusion-limited range" interfere with the copper reduction, promoting the competitive hydrogen production. The current density value for a given bath for which the second plateau occurs is the most interesting.

According to Sand et al.[25] (Equation 1), it is possible to calculated a physical quantity characteristic of the time required to reach diffusion limit for a specific applied current pulse (Table II).

$$\tau = \frac{\pi D_{Cu}\, C_{Cu}^2 (zF)^2}{4\, J_c^2} \qquad [1]$$

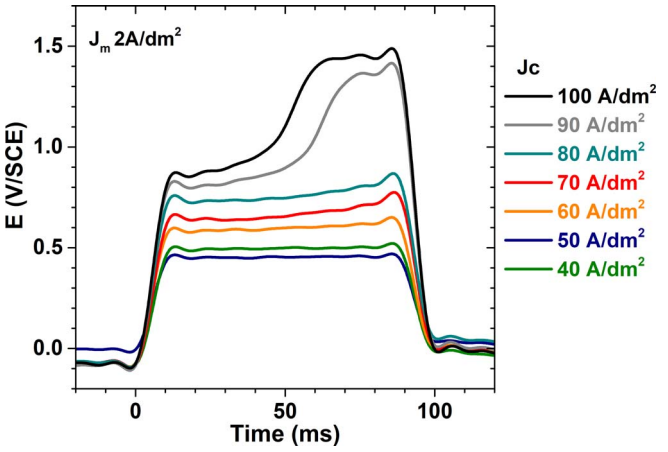

Figure 3. Transient curves in response to different cathodic currents (40–100 A dm^{-2}) for a fixed T_{on} = 100 ms, and constant $I_{average}$ = 2 A dm^{-2} recorded for the bath with d-xylose.

Table II. Transition time for the single pulses.

Jc (A/dm^2)	40	50	60	70	80	90	100
τ (ms)	217	139	96	71	54	43	35

Where D_{Cu} is the diffusion coefficient of copper in copper sulfate sulfuric acid solutions (5.59×10^{-6} cm^2 s^{-1}), C_{Cu} is the copper concentration in the solution (0.46 M), J_c is the cathodic current density, *F* is the Farady constant (96 485 C mol^{-1}) and z is the number of electrons taking part in the reduction reaction

It is interesting to note that, for the lower current densities i.e. 40 or 50 A/dm^2, τ values are much higher than the pulse durations. In these cases this means that the pulse sequence could have included a longer t_{on}, without changes in potential value. The transition occurs around 60 A/dm^2, but the τ decrease is less and less pronounced as the current density increases. When adding 33 mg/L of d-xylose, higher current densities may be reached before the occurrence of the transition between the faradaic reduction of copper, near the electrode, and the diffusion-limited mechanism. τ values were not calculated in the case of d-xylose presence because of the uncertainty on diffusion coefficient rate.

As a result of the above, four singular situations have been selected on the curves related to typical patterns, including or avoiding the "diffusion-limited range" plateau: the pulse sequences (40 A dm^{-2}, T_{on} = 20 ms), (40 A dm^{-2}, T_{on} = 80 ms), (70 A dm^{-2}, T_{on} = 20 ms) and (70 A dm^{-2}, T_{on} = 80 ms). These were used to prepare samples for characterization in terms of hydrogen outgassing by TDS and XRD measurements. Off-time was adjusted to keep the same constant average current of 2 A dm^{-2} and the pulse parameters are given in Table III. From the table is clear that increasing T_{on} increases also T_{off}, since the average current density is kept constant.

Due to very long off-times, we checked the interface behavior in absence of current. According to the performed tests, copper dissolution in the copper plating bath is negligible, because weight measurement doesn't show any variation even after hours of exposure. In the same manner, adsorption of D-xylose which may occur during off-times is also not related to reaction inhibition, as the corresponding polarization curves do not show an additional shift in the reduction potential. On the contrary, for the potential where copper reduction occurs, current densities in presence of xylose are always slightly higher than in absence of additive. Finally, surface tension of the electrolyte was also investigated as it was sought the possible contribution of wettability modification[32] by d-xylose in inhibiting the hydrogen to adsorb onto the growing crystals or modifying the formation of bubbles in solution. The surface tension was measured by the stalagmometric method for the two electrolytes and revealed similar value for both cases of 74.5 ± 0.5 mN/m.

Measurement of hydrogen content by thermal desorption spectroscopy.—All electroformed samples followed the same production process. At the first stage of the process, aluminum flat parts were copper-coated on one side to provide an adherent layer for the subsequent plating. Flat aluminum samples of 2.5 cm × 2.5 cm, AW-1050 alloy, 99.5% purity, were copper-coated at room temperature via magnetron sputtering using a cathode-substrate distance of 200 mm with an average power of 380 W, and using Kr as the sputtering process gas at a working pressure of about 7×10^{-4} mbar to deposit ~3 μm of copper layer. Afterwards, the samples were masked on the external side and plated for 24 hours at an average current density of 2 A dm^{-2} in order to achieve a theoretical thickness of 634 μm following the respective pulse sequence for the two different electrolytes. Finally, the electroformed copper layer was peeled off from the aluminum flat parts. The mass of copper deposited may vary, following the Faradic efficiencies which may vary as a function of the different current intensities. Therefore, TDS samples of 10 mm x 10 mm were extracted from larger plated samples. Prior to all measurements, the samples were weighted, with an accuracy of 0.1%, in order to calculate the corresponding normalized outgassing and concentration.

Table III. Pulse parameters for the TDS samples.

	Ton [ms]	Toff [ms]
40 A/dm^2	20	380
40 A/dm^2	80	1520
70 A/dm^2	20	680
70 A/dm^2	80	2720

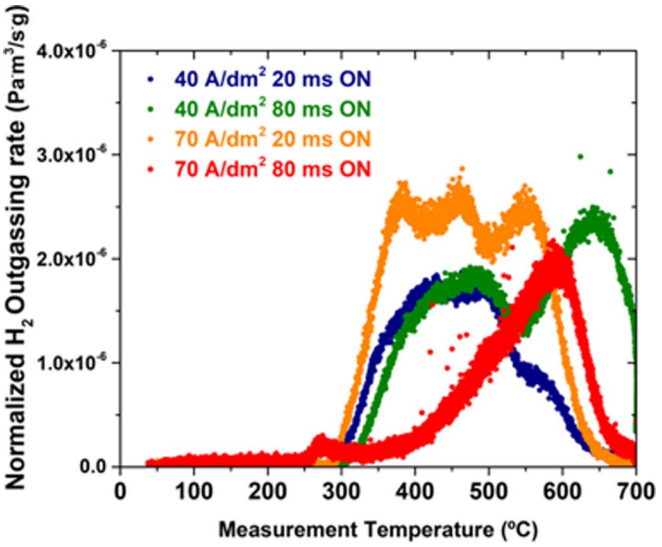

Figure 4. Normalized H_2 outgassing rate as a function of heating temperature for the 4 different pulse sequences in the bath without additives: 40 A dm^{-2}, 20 ms (in blue) and 80 ms (in green) cathodic time and 70 A dm^{-2} cathodic time, 20 ms (in orange) and 80 ms (in red), with average current of 2 A dm^{-2} in all cases.

H_2 outgassing was measured for the different plated samples (heating rate 10°C/min, from 20°C to 700°C), and the results are shown in Figures 4 and 5. To avoid self-annealing risks,[26] samples were analyzed

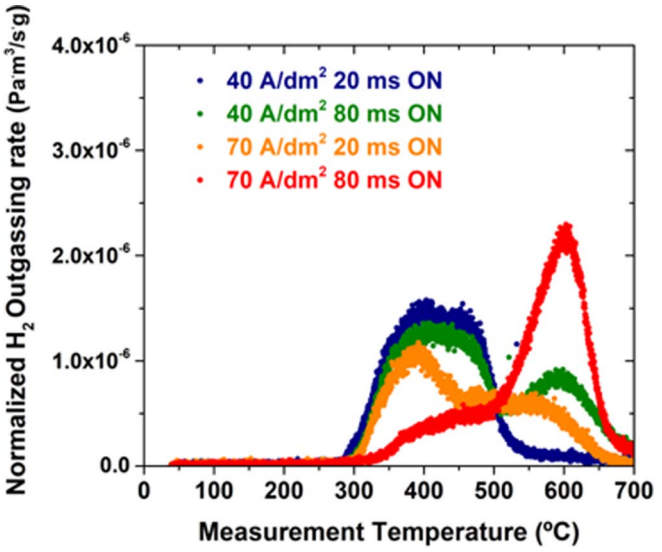

Figure 5. Normalized H_2 outgassing rate as a function of heating temperature for the 4 different pulse sequences in the bath with d-xylose: 40 A dm^{-2}, 20 ms (in blue) and 80 ms (in green) cathodic time and 70 A dm^{-2}, 20 ms (in orange) and 80 ms (in red) cathodic time, with average current of 2 A dm^{-2} in all cases.

within hours after plating. H_2 outgassing rate is plotted as a function of heating temperature for each plating sequence and each electrolyte and the total concentration (at. ppm) is calculated by weighting the sample before each TDS measurement.

In Figures 4 and 5, two different outgassing peaks (regions) are identified. The first peak occurs between 300°C - 500°C, while the second peak evolves at higher temperatures (600°C - 700°C). Approximately the same two peaks were found by Gubin et al.[7] (450°C and 600°C) on thin electroplated films of some tens of μm, and as in the present case the high temperature peak was particularly marked for high current. Some authors[7,29] suggest that hydrogen is stored in the material in two forms: atomic hydrogen in solid solution in thermal equilibrium (i.e. representing the solubility), certainly at very low level and under the TDS detection limit or atomic hydrogen above solubility in vancancies, and molecular hydrogen, which may be located at the grain boundaries or defects. Fukai et al.[27,28] also observed different outgassing peaks in their study of super vacancy hydrogen formation in copper. The super-vacancies occur in electrodeposition as M-H atoms and M-atom vacancies are deposited by atom-by-atom process.[26] The nature of the first peak can be ascribed to hydrogen diffusion from vacancies and is largely described in literature.[6–8] Hydrogen is produced during electroplating as a side reaction and several atoms can replace the position of a copper atom in the lattice. The second peak is not fully understood. Fukai et al.[28] suggest two different possible explanations for the high temperature peak. The first explanation is that it originates from precipitation of H from the vacancies in hydrogen bubbles that will undergo higher diffusion resistance in the copper lattice. The second explanation is that hydrogen can create super abundant vacancies with a higher number of H atoms sharing a vacancy site.

From the metallurgy point of view if we consider the behavior of copper during thermal treatment, the temperature of annealing (reduction of the mechanical properties) for cold rolled is about 220°C for 15 minutes of treatment, but can shift up to 400°C in absence of cold working.[30] The fact that electrodeposited copper can be considered as not cold worked and that the temperature during the TDS measurement is following a fast ramp at 10°C/minute makes plausible that the first peak corresponds to annealing of the sample. The second peak at much higher temperature corresponds to the range where a grain growth occurs.

For the d-xylose bath (Figure 5), we can follow the effect of increasing cathodic time on the outgassing trend (for 40 A dm^{-2}: 20 ms and 80 ms). For short pulses, hydrogen is mainly outgassed in the first peak (300°C-500°C), while for long pulses it is additionally released around 600°C.

For the no-additive case (Figure 4), the same trend is observed. Moreover, the samples that were plated at higher current and higher pulse time (in this case this sample is in the limited diffusion plateau of Figures 2), only exhibit the second peak at 600°C and the first peak is absent.

In conclusion, data presented in Figures 4 and 5 demonstrate that the pulse length influences the hydrogen trapping mode into the material. In the explored range of current density values, for both cases - with and without additive - the samples produced with pulses with longer T_{on} exhibit a larger proportion of hydrogen in the higher temperature peak of desorption (around 600°C), compared to the samples with shorter T_{on}, where hydrogen desorbs mainly at lower temperature. As mentioned above, such two peaks were interpreted by other authors as belonging to different species of hydrogen incorporated in copper [8]. We remark that displacing the hydrogen to a state which contributes to outgassing only at very high temperature would be beneficial for electroformed vacuum chambers, which are used in a temperature range below 300°C [4].

In order to compare the quantities of hydrogen released, the concentration (at. ppm) is calculated as per Equation 2, integrating the total amount of outgassed hydrogen, and is plotted versus the pulse charge density per period ($J_{on}xT_{on}$) as seen in Figure 6 and Table V

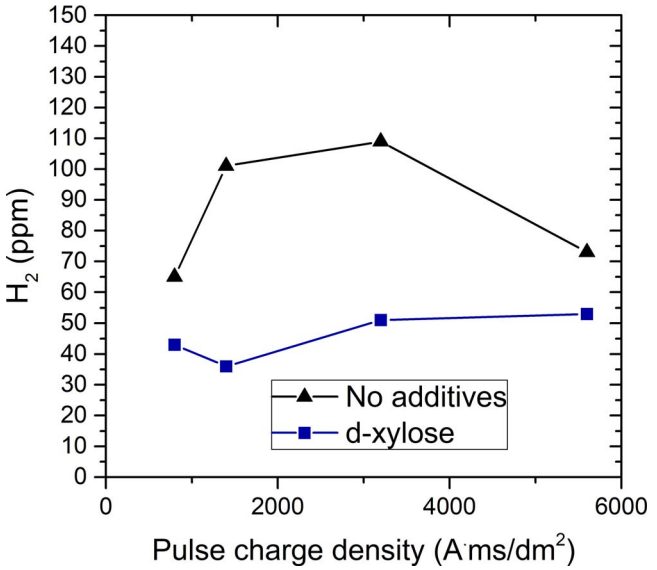

Figure 6. H_2 concentration into the coating (atomic ppm) as a function of pulse charge density per period ($J_{on}xT_{on}$). The two electrolytes are compared.

below.

$$H_2(\text{atomic ppm}) = \frac{mol\ H_2\ outgassed}{10^{-6}\ \text{mol Cu total}} \quad [2]$$

Comparing the quantitative results of H_2 incorporation as a function of pulse charge density in the absence of additive, it can be assumed that the incorporation of hydrogen is proportionally to its generation. This is true for the following sequences (40 A dm^{-2}, T_{on} = 20 ms) < (70 A dm^{-2}, T_{on} = 20 ms) < (40 A dm^{-2}, T_{on} = 80 ms). But one sequence (70 A dm^{-2}, T_{on} = 80 ms), doesn't fit into this scheme. This sequence is the single one of the test panel which presents a "diffusion-limited range" plateau. During electroplating, strong hydrogen bubbling for this sample was noticeable, which confirmed high hydrogen generation. Outgassing results (Figure 4) evidenced a dominant outgassing peak at 600°C. The high level of hydrogen generation in this case is also accompanied with higher disturbances of the limiting diffusion zone, which will favor bubble coalescence and hydrogen removal from the interface.

Thus, from the data in Figure 6 we conclude that the incorporation mechanism seems to play an important role in addition to the production of H in the bath. We compared the amount of plated copper per pulse in each case, just by scaling from the total plated amount, and we compared it with the diffusion length during the time T_{off} by using the diffusion coefficient D of H in copper at room temperature, extracted from Nakamura.[33] The comparison is shown in Table V.

It is clear that the diffusion length is in all cases very large compared to the thickness per pulse, meaning that H dissolved in copper would have the time to move across the layer, diffuse in and out. This phenomenon is independent of the time-off duration, because even at 10-times smaller T_{off} values, hydrogen would have already left the coating by diffusion. This would result in an equilibrium concentration of H corresponding to the solubility limit[34] in all cases, but would not explain the different amounts outgassed in TDS. Therefore, it confirms that the hydrogen is incorporated in a different state and cannot diffuse easily. All the values of concentration found in the samples are above the solubility limit and this clearly demonstrates that we incorporate hydrogen in bound states in addition to the hydrogen dissolved in copper. This is consistent with the conclusions from Figures 4 and 5 which indicates that the hydrogen trapping states are different for the long and short pulse times.

As a result of comparing H_2 concentration on samples from the d-xylose bath and the non-additive bath (see Figure 6 and Table IV), we could confirm the role of d-xylose as an inhibitor for H incorporation

Table IV. Hydrogen concentration, in atomic ppm, as measured by TDS.

Plating parameters	Bath without additives	Bath with d-xylose
40 A/dm^2, T_{on} = 20 ms	65	42
40 A/dm^2, T_{on} = 80 ms	109	51
70 A/dm^2, T_{on} = 20 ms	101	37
70 A/dm^2, T_{on} = 80 ms	73	53

into the deposit. Indeed, all the samples without the additive show a higher hydrogen content than those with xylose and this is independent of the pulse parameters. The results match with previous studies conducted with d-xylose as an additive on the copper sulfate plating bath, where the same hydrogen evolution was observed at longer times.[12,21] Other authors[12,31] reported a H concentration of 1 wt ppm (31 at. ppm for H_2) for a copper sulfate bath containing d-xylose as additive, and values 10 times higher for an acidic $CuSO_4$ bath without additives.

It is interesting to link the electrochemical behavior in presence of d-xylose to the reduction of hydrogen concentration into the coating. Looking closely to the outgassing rates (Figure 5), one can notice that for the lowest pulse charge density (40 A dm^{-2}, T_{on} = 20 ms), the outgassing is restricted to the first peak, at 300°C–500°C, ascribed to hydrogen diffusion from vacancies. Then, increasing the pulse length or the current density, the second peak at 600°C appears and grows resulting from a second mode of hydrogen storage in super abundant vacancies or bubbles at grain boundaries, which may be considered as defects. The latest's are already present in absence of d-xylose for the lowest pulse charge density and in a more significant manner for the other pulse charge densities as shown in Figure 4, suggesting a less efficient copper reduction. This is in agreement with CV curves (Figure 1) where the current density in presence of d-xylose is always higher. It is also in agreement with the transient curves (Figure 3) where the emergence of the "diffusion-limited range" plateau is delayed at higher current density. This confirms that copper reduction is favored due to d-xylose adsorption.

Table V. thickness deposited per pulse and diffusion length of H in copper during T_{off}.

Plating parameters	Thickness per pulse [nm]	$(D*T_{off})^{1/2}$ [nm]
40 A/dm^2, T_{on} = 20 ms	2.4	267
40 A/dm^2, T_{on} = 80 ms	9.2	534
70 A/dm^2, T_{on} = 20 ms	2.6	357
70 A/dm^2, T_{on} = 80 ms	11.2	714

Microscopic studies.—After the outgassing measurements, the samples were characterized by microscopy analysis. Figure 7 displays the SEM images of electroformed copper samples in the bath without additives (a) and in the bath with d-xylose (b), keeping the same average current density 2 A dm^{-2} by adjusting T_{off}. After SEM imaging the measurement of the grain size was performed after polishing (removing 10–20 μm of the top surface) and micro-etching (according to ASTM E112) of the surface.

From the SEM observations of Figure 7, the differences between the deposited layers from the two different electrolytes are less noticeable than those for the different pulse plating sequences. The influence of the presence (or absence) of d-xylose was already found to have limited effects on mechanical properties or microstructure as shown by Malone et al.[21] whereas increasing the average current density from 40 to 70 A dm^{-2} is of primary influence.

The differences in grain size between both electrolytes for the same set of parameters (current density and Ton) are detailed in Figure 8. For both bath compositions, when the current density increases for a fixed T_{on} (Figures 7 and 8: the pair a1-a3 and b1-b3, for instance), the nucleation rate increases and thus does the number of grains per surface area, resulting in a smaller grain size.[35] This is explained by Ibl et al.[36] by the fact that the activation overpotential becomes larger with increasing current density, so that larger free energy is available which allows the formation of new nuclei. They reported similar conclusions in their study of the pulse parameters effect on the grain morphology of Cd deposits from sulfate baths.

For the 40 A dm^{-2} current density, there is no significant tendency when changing the on-time. In the case of 70 A dm^{-2}, an increase in pulse time T_{on} leads to an increase of the average grain size (Figures 7 and 8: compare a3 with a4 and b3 with b4). This might be explained by the fact that for fixed current density a longer T_{on} enables a larger

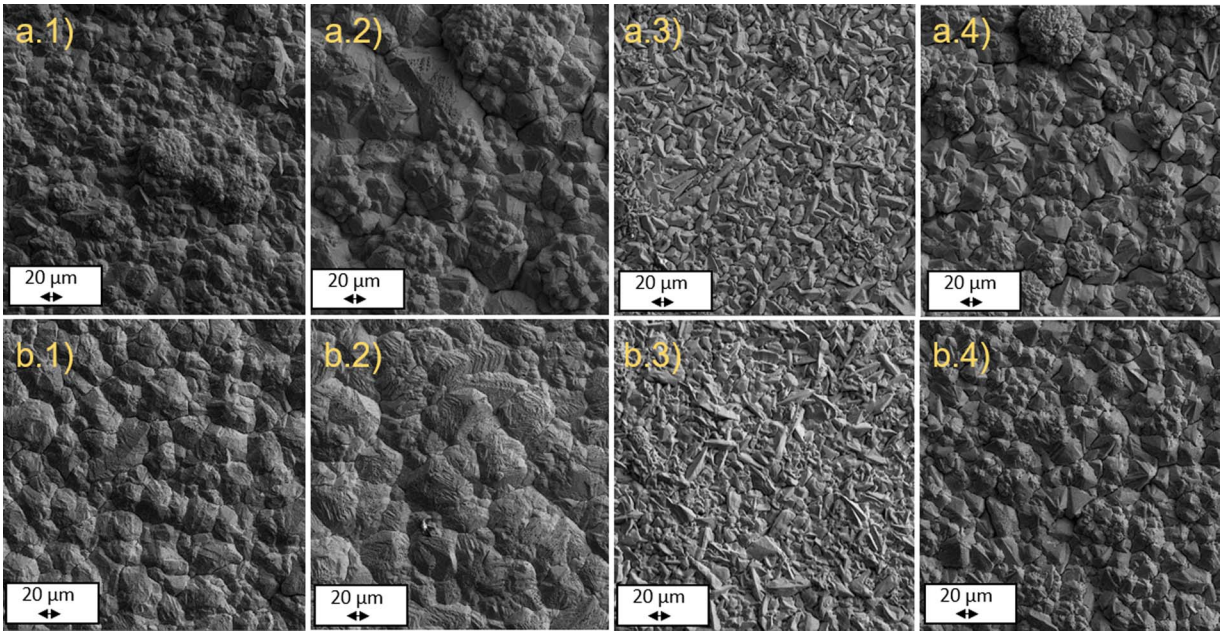

Figure 7. SEM pictures of electroformed copper using different pulse sequences 1: 40 A dm^{-2}, T_{on} = 20 ms, 2: 40 A dm^{-2}, T_{on} = 80 ms, 3: 70 A dm^{-2}, T_{on} = 20 ms, (4): 70 A dm^{-2}, T_{on} = 80 ms. Average current density is kept at 2 A dm^{-2} by adjusting off-time. Samples from the non-additive bath (a) and the d-xylose bath (b) are compared.

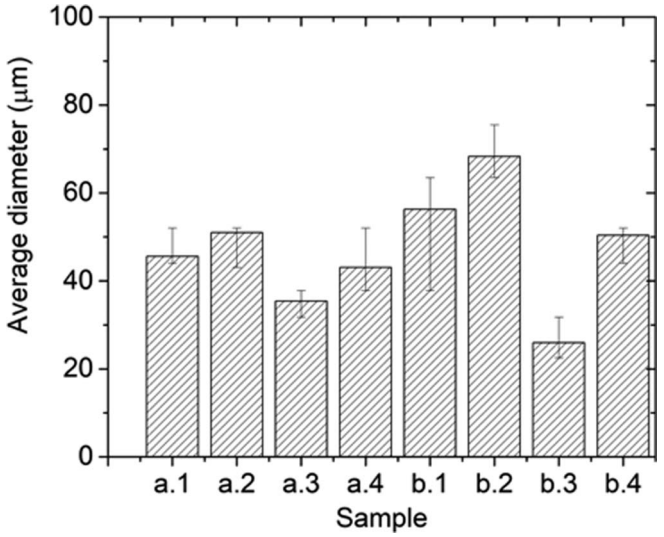

Figure 8. Grain size from the metallographic observation (average (µm) and absolute errors). for 1: 40 A dm^{-2}, $T_{on} = 20$ ms, 2: 40 A dm^{-2}, $T_{on} = 80$ ms, 3: 70 A dm^{-2}, $T_{on} = 20$ ms, (4): 70 A dm^{-2}, $T_{on} = 80$ ms. Average current density is kept at 2 A dm^{-2} by adjusting off-time. Samples from the non-additive bath (a) and the d-xylose bath (b) are compared.

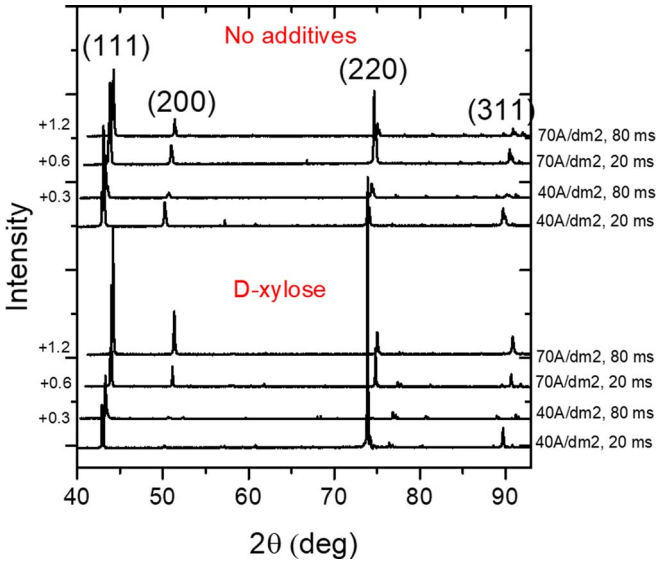

Figure 9. X-ray diffractograms of copper-plated samples produced at different pulse sequences for the two electrolytes at room temperature.

amount of material to be deposited continuously onto a grain during each pulse before adsorption of impurities during T_{off}. Such impurities might induce formation of defects setting a limit to grain growth. This effect is more marked at higher current density since more material is deposited in each pulse. The SEM pictures also show the presence of cracks after outgassing for the higher pulse charge density (In Figure 7, a.4 and b.4). These samples mainly exhibited the second outgassing peak at 600°C during heat-treatment. A possible interpretation for the cracks is that they were produced during release of hydrogen, which accumulates in bubble form on the grain boundaries.[29]

Microstructure and preferred orientation by X-Ray diffraction analysis (XRD).—XRD analysis was performed on twin electroformed samples in order to study the microstructure of the samples. Diffractograms were recorded at room temperature and after in-situ heating at different temperature plateaus (20°C, 300°C, 500°C and 700°C) at a heating ramp of 10°C/min. Characteristic copper diffraction peaks corresponding to planes (111), (200), (220) and (311) were observed as shown in Figure 9. For these samples, we can see a difference in the relative intensities of the various orientations. This can be quantified by calculating the relative proportion of the intensities for different crystallographic planes (h,k,l) in Equation 3, where $I_{(h,k,l)}$ are peak intensities on the diffraction patterns and $I_{0(h,k,l)}$ are the theoretical ones (taken from JCPDS 070–3038 for Cu) for an isotropic sample.

$$RTC = \frac{I_{hkl}/I^0_{hkl}}{\sum I_{hkl}/I^0_{hkl}} \quad [3]$$

The relative texture coefficient is compared for different pulse charge densities in Figure 10. In the absence of additives, the preferential orientation for (220) plane decreases while the pulse charge density increases, and nearly all samples show a similar preference for planes (200), (111) and (311). As the applied current density increases, the nucleation rate increases and thus the probability of grains oriented randomly in different planes.[35] This was already observed by Marro et al.[14] for RTC values as a function of pulse on-time decrease. They report that an increase in pulse time is followed by a decrease in preferential orientation. They correlated this fact to the increase of residual stress in copper films.

In presence of d-xylose, samples with lower charge density exhibited a very strong relative preferential orientation of 0.9 for the plane (220). However, this preference decreases when charge density increases. For the highest charge density values, the plane orientation is more randomly distributed, which may be linked to SEM observations presenting a better grain homogeneity. This kind of behavior as already been observed[20] i.e. the attenuation of preferential orientation by pulsed current in additive presence, even if the preferential planes are specific to the electrolytes used.

In Figure 11, the lattice parameter is plotted vs. the heating temperature. As no clear influence of the additive presence has been noticed, the figure does only make the distinction between pulse sequences (short and long T_{on} times). Increasing the temperature leads to an increase of the lattice parameter of pure copper, due to thermal expansion. The simultaneous release of hydrogen during the heating, normally resulting in a contraction of the microstructure by vacancy migration or atomic positional shifts on other complex systems,[37] is not sufficient to counterbalance this phenomenon and the variation of pure copper is globally positive (dots and black line on Figure 11, data extracted from literature).[38,39] However, if the lattice parameter variation is consistent with the values from the literature between 25°C and 300°C, a difference arises above 450°C. From there, the value of the lattice parameter stops increasing, which can be attributed to a more significant microstructure reorganization, due to H_2 vacancy diffusion. This must be seen in view of the outgassing measurement results, where two kinds of degassing peaks were reported: one centered around 400°C and the other about 600°C, representative of two kind of hydrogen trapping mode. The discrepancies found with the pure copper data can also be accounted for by the presence of a specific trapped hydrogen form, because it occurs above the temperature threshold. This is confirmed by the fact that longer pulses always exhibit a larger lattice parameter mismatch than shorter pulses, corresponding to the higher hydrogen outgassing level around 600°C.

These results should nevertheless be viewed cautiously, because the presence of other impurities such as carbon in the bulk or oxides on the surface may interfere into the measurements.

Conclusions

With the view to reduce the impurities and especially the gas trapped during electroforming of thick copper layers, two parameters have been evaluated: current modulation by changing pulse duration and magnitude, and presence or absence of a chemical additive. In keeping with transient curves, addition of d-xylose reduced H content in the deposit. D-xylose addition did not cause significant

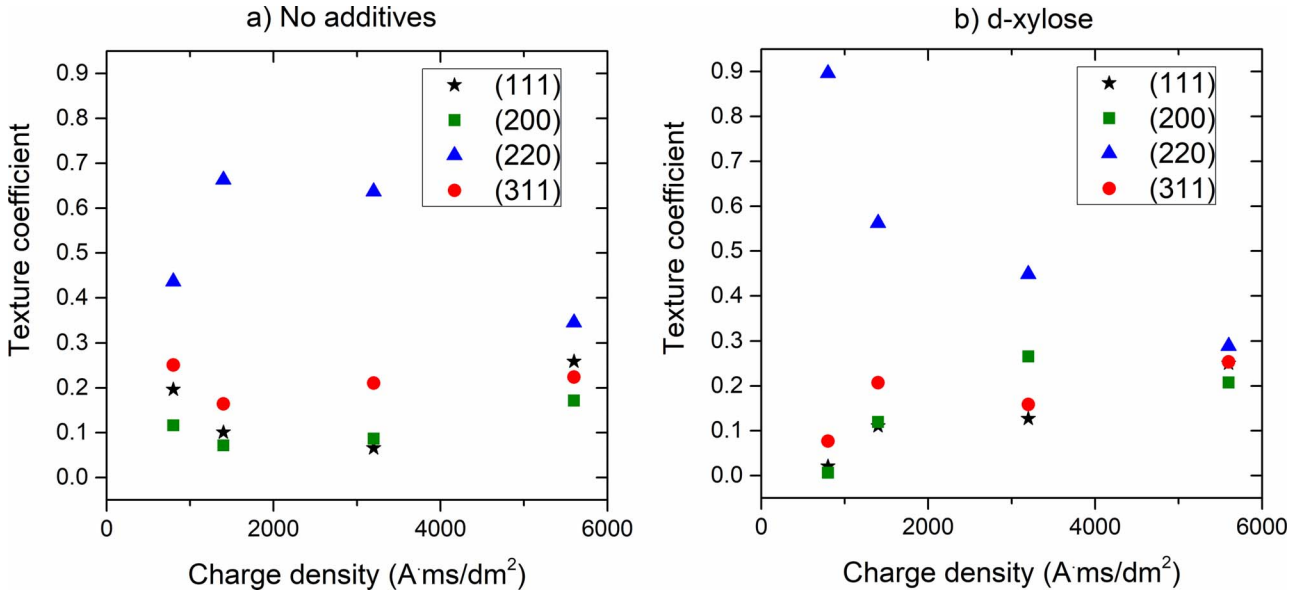

Figure 10. Relative texture coefficient of copper-plated samples as a function of pulse charge density per period ($J_{on}xT_{on}$). Samples from the non-additive bath (a) and d-xylose bath (b) are compared.

changes in microstructure and led to a more strongly-oriented growth. H_2 outgassing results revealed different H-trapping states on the electroformed copper. One is ascribed to atomic hydrogen contained in copper vacancies, while the other could be interpreted by hydrogen trapped in other forms. Increasing pulse time led to the presence of a high temperature desorption peak in addition to the primary desorption peak, which is at around 400°C. This is particularly surprising as it means that, even if no secondary plateau due to diffusion-limited range is observed, a high content of hydrogen can be trapped for longer pulse times. At the contrary, the situation expected to lead to an intense hydrogen incorporation (higher current densities for longer times) does not lead to that high content. A sequence can be specifically designed in which H_2 degassing occurs only at very high temperatures. This could be convenient when applied to vacuum chamber electroforming. Furthermore, the microstructure is also dependent on the chosen pulse. Future steps will consist in an optimization of bath composition with respect to the outgassing, by varying $CuSO_4$ or H_2SO_4 concentration in the bath[40] or by adding different additives. Additionally, reverse pulse current may be a promising technique for further investigation and fabrication of very pure copper deposits.

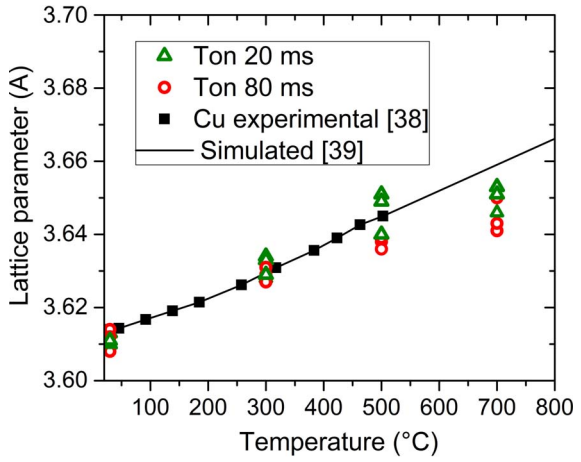

Figure 11. Lattice parameter evolution with increasing temperature from 20°C to 700°C with a 10°C/min step for the different pulse sequences. Short pulses (20 ms) are represented in green (Δ) and long pulses (80 ms) in red (○). The data are compared with reference copper reported values.[38,39]

Acknowledgments

This research is part of a project within a collaboration between CERN and the Institute UTINAM (Université de Bourgogne Franche-Comté/CNRS) and is supported by CERN. The authors would like to thank E. Garcia-Tabares for the SEM images.

ORCID

J-Y Hihn https://orcid.org/0000-0002-7857-2098

References

1. C. Steier, A. Anders, D. Arbelaez, J. M. Byrd, K. Chow, S. De Santis, R. M. Duarte, J.-Y. Jung, T. H. Luo, A. Madur, H. Nishimura, J. R. Osborn, G. C. Pappas, L. R. Reginato, D. Robin, F. Sannibale, D. Schlueter, C. Sun, C. A. Swenson, W. L. Waldron, E. J. Wallen, and W. Wan, *in* "Proceedings of IPAC", p. 1840, Richmond, USA, 2015.
2. C. Benvenuti, P. Chiggiato, F. Cicoira, and Y. L'Aminot, *J. Vac. Sci. Technol., A*, **16**, 148 (1998).
3. P. Chiggiato and P. Costa Pinto, *Thin Solid Films*, **515**(2), 382 (2005).
4. L. Lain Amador, P. Chiggiato, L. M. A. Ferreira, V. Nistor, A. T. Perez Fontenla, M. Taborelli, W. Vollenberg, M.-L. Doche, and J.-Y. Hihn, *J. Vac. Sci. Technol. A*, **36**(2), (2018).
5. C. Benvenuti, *in* "Proceedings of PAC", p. 602, Chicago, USA, 2001.
6. J. C. Farmer et al., *Plating Surf. Finish.*, **75**(48), (1988).
7. V. V. Gubin, L. T. Zhuravlev, B. M. Platonov, and Y. M. Polukarov, *Soviet Electrochem.*, **20**(5), 671 (1984).
8. N. Fukumuro, T. Adachi, S. Yae, H. Matsuda, and Y. Fukai, *Transactions of the IMF*, **89**(4), 198 (2011).
9. W. Metzger, E. Knaak, and J. Hupe, *Plating Surf. Finish.*, **75**(64), (1998).
10. N. V. Shanmugam and S. J. P. Thangavelu, *Trans. Met. Finish. Assoc*, **27**, (1994).
11. R. D. Srivastava and S. Kumar, *Trans. Inst. Met. Finish*, **50**(102), (1972).
12. J. W. Dini, *Thin Solid Films*, **95**(2), 123 (1982).
13. N. Tantavichet and M. D. Pritzker, *Electrochimica Acta*, **50**(9), 1849 (2005).
14. J. B. Marro, T. Darroudi, C. A. Okoro, Y. S. Obeng, and K. C. Richardson, *Thin solid films*, **621**, 91 (2017).
15. W. E. G. Hansel and S. Roy, *Pulse Plating*, Leuze Verlag KG, Bad Saulgau, Germany (2012).
16. F. Lallemand, L. Ricq, E. Deschaseaux, L. de Vettor, and P. Bercot, *Surface & Coatings Technology*, **197**(1), 10 (2005).
17. J. Cl. Puippe and N. Ibl, *J. Appl. Electrochem.*, **10**, (1980).
18. E. J. Taylor, C. Zhou, and J. J. Sun, Pulse reverse electrodeposition for metallization and planarization of semiconductor substrates, USPTO Pat. Grants, 2005.
19. E. J. Taylor and M. E. Inman, Electrodeposition of catalytic metals using pulsed electric fields, USPTO Pat. Grants, 2000.

20. E. M. Dela Pena and S. Roy, *Surf. Coat. Technol.*, **339**, (2018).
21. G. A. Malone, W. Hudson, B. Babcock, and R. Edwards, Improved Electroformed Structural Copper and Copper Alloys, NASA/CR–1998-20868, 1998.
22. J. R. Denchfield, Process for electroforming low oxygen copper, US3616330A, 1971.
23. E. Herrero, L. J. Buller, and H. D. Abruna, *Chem. Rev.*, 101, (2001).
24. S. Brankovic, J. Wang, and R. Adi, *Surf. Sci.*, **474**(1), 173 (2001).
25. H. J. S. Sand, Phis. Mag., **1**(1), (1901).
26. Y. Fukai, *Defect and Diffusion Forum*, **312–315**, 1106 (2011).
27. Y. Fukai, *Journal of Alloys and Compounds*, **356–357**, 263 (2003).
28. Y. Fukai, M. Mizutani, S. Yokota, M. Kanazawa, Y. Miura, and T. Watanabe, *Journal of Alloys and Compounds*, **356–357**, 270 (2003).
29. A. Martinsson and K. Swerea, Hydrogen in oxygen-free, phosphorus-doped copper, IAEA report SKB-TR–13-09 (2013).
30. J. R. Davis, ASM Specialty Handbook, Copper and Copper Alloys, ASM international, Materials Park (2001).
31. F. T. Schuler, H. A. Tripp, and M. J. Mullery, Electrodeposited copper for elevated temperature usage, Copper Development Association-American Society for Metals Conf. on Copper, Cleveland, OH (1972).
32. C. W. Liu, J. C. Tsao, M. S. Tsai, and Y. L. Wang, *J. Vac. Sci. Technol. A*, **22**(6), 2315 (2004)
33. H. Nakamura, S. O'hira, W. Shu, M. Nishi, T. J. Venhaus, R. A. Causey, D. R. Hyatt, and R. S. Willms, *J. Nucl. Mater.*, **283–287**(2), 1043 (2000).
34. H. Wipf, *Physica Scripta*, **94**(1), 43 (2001).
35. A. M. Rashidi and A. Amadeh, *J. Mater. Sci. Technol.*, **26**(1), 82 (2010).
36. N. Ibl, J. Cl. Puippe, and H. Angerer, *Surface Technology*, **6**(4), (1978)
37. S. A. Acharya, V. M. Gaikwad, V. Sathe, and S. K. Kulkarni, *Applied Physics Letters*, **104**(11), 113508 (2014).
38. F. C. Nix and D. MacNair, *Physical Review*, **60**(8), 597 (1941).
39. C. Q. Sun, An approach to local band average for the temperature dependence of lattice thermal expansion, arXiv:0801.0771, 2008.
40. C. Shen, Z. Zhu, D. Zhu, and J. Ren, *J. Mater. Eng. Perform.*, **26** (2017).